Synergistic Combination of Multi-Zr^IV Cations and Lacunary Keggin Germanotungstates Leading to a Gigantic Zr24-Cluster-Substituted Polyoxometalate

Ling Huang,[†] Sa-Sa Wang,[†] Jun-Wei Zhao,*[,‡] Lin Cheng,[†] and Guo-Yu Yang*[,†]

[†]State Key Laboratory of Structural Chemistry, Fujian Institute of Research on the Structure of Matter, Chinese Academy of Sciences, Fuzhou, Fujian 350002, China

[‡]Henan Key Laboratory of Polyoxometalate Chemistry, College of Chemistry and Chemical Engineering, Henan University, Kaifeng, Henan 475004, China

S *Supporting Information*

ABSTRACT: Synergistic directing roles of six lacunary fragments resulted in an unprecedented Zr24-cluster substituted poly(polyoxotungstate) $Na_{10}K_{22}[Zr_{24}O_{22}(OH)_{10}(H_2O)_2(W_2O_{10}H)_2(GeW_9O_{34})_4(GeW_8O_{31})_2] \cdot 85H_2O$ ($Na_{10}K_{22} \cdot \mathbf{1} \cdot 85H_2O$), which contains the largest $[Zr_{24}O_{22}(OH)_{10}(H_2O)_2]$ (Zr_{24}) cluster in all the Zr-based poly-(polyoxometalate)s to date. The most remarkable feature is that the centrosymmetric Zr24-cluster-based hexamer contains two symmetry-related $[Zr_{12}O_{11}(OH)_5(H_2O)(W_2O_{10}H)(GeW_9O_{34})_2(GeW_8O_{31})]^{16-}$ trimers via six μ_3-oxo bridges and was simultaneously trapped by three types of different segments of B-α-GeW_9O_{34}, B-α-GeW_8O_{31}, and W_2O_{10}. The other interesting characteristic is that there are two pairs of intriguing triangular atom alignments: one is composed of the Zr(2,4,6,8,11) and W21 atoms and the other contains the Ge(1−3), Zr(3,5,7,9,10,12) and W26 atoms, and the Zr5 atom is inside the triangle; a linking mode is unobserved. The oxygenation reactions of thioethers by H_2O_2 were evaluated when $Na_{10}K_{22} \cdot \mathbf{1} \cdot 85H_2O$ served as a catalyst. Results show that it is an effective catalyst for oxygenation of thioethers by H_2O_2. The unique redox property of oxygen-enriched polyoxotungstate fragments and Lewis acidity of the Zr cluster imbedded in $Na_{10}K_{22} \cdot \mathbf{1} \cdot 85H_2O$ provide a sufficient driving force for the catalytic conversion from thioethers to sulfoxides/sulfones.
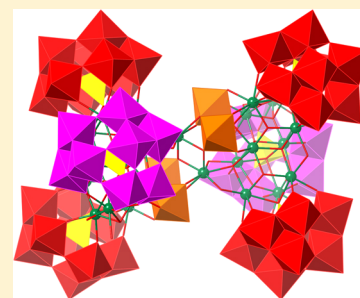
INTRODUCTION

Polyoxometalates (POMs) coupled with their rich electronic properties and molecular characteristics have realized applications in diverse fields such as catalysis, medicine, and magnetism.[1] Currently, the design and synthesis of unique POMs with a higher number of transition metal (TM) centers are predominantly driven by their catalytic and magnetic properties as well as structural aesthetic appreciation. To date, TM cluster incorporated polyoxotungstates (POTs) are now well-established and numerous giant-cluster-based poly(POT)s have been made such as $[Mn_{19}(OH)_{12}(SiW_{10}O_{37})_6]^{34-}$,[2a] $[H_{56}Fe_{28}P_8W_{48}O_{248}]^{28-}$,[2b] $[\{Co_4(OH)_3PO_4\}_4(PW_9O_{34})_4]^{28-}$,[2c] $[Cu_{20}Cl(OH)_{24}(H_2O)_{12}(P_8W_{48}O_{184})]^{25-}$,[2d] $[Nb_4O_6(\alpha\text{-}Nb_3\text{-}SiW_9O_{40})_4]^{20-}$,[2e] $[(P_2W_{15}Ti_3O_{62})_4\{Ti(OH)_3\}_4Cl]^{45-}$,[2f] $[(P_8W_{48}O_{184})\{(P_2W_{14}Mn^{III}_4O_{60})(P_2W_{15}Mn^{III}_3O_{58})_2\}_4]^{152-}$,[2g] $[(NH_4)_{20}[\{(W)W_5O_{21}(SO_4)\}_{12}\{(Fe^{III}(H_2O))_{30}\}(SO_4)_{13}(H_2O)_{34}]]^{12-}$,[2h] and $[\{Ni^{II}_6(Tris)(en)_3(BTC)_{1.5}(B\text{-}\alpha\text{-}PW_9O_{34})\}_8]^{36-}$;[2i] however, the analogous chemistry of zirconium is less developed, though the Zr-based POTs possess useful catalytic properties.[3a−c] Since the first Zr-based POT $[Zr_3(\mu_2\text{-}OH)_3(A\text{-}\beta\text{-}SiW_9O_{34})_2]^{11-}$ was made in 1989,[3d] so far the maximum number of Zr atoms in substituted POTs is only six as observed in $[Zr_6O_2(OH)_4(H_2O)_3(\beta\text{-}SiW_{10}O_{37})_3]^{14-}$,[3e] $[Zr_6(O_2)_6(OH)_6(\gamma\text{-}SiW_{10}O_{36})_3]^{18-}$,[3f] and $[Zr_6O_4(OH)_4(H_2O)_2(CH_3COO)_5(AsW_9O_{33})_2]^{11-}$.[3g] Thus, exploring giant Zr-

cluster incorporated POTs and evaluating catalytic properties remain a great challenge. Whether the giant Zr-cluster can be incorporated to lacunary POT skeletons is very interesting and challenging topic.

All the above poly(POT)s are generally prepared by reaction of multilacunary POT precursors with TM ions under conventional solutions. Recently, the hydrothermal method has been used by our lab to make TM-substituted POTs in the reaction systems of lacunary POT fragments and divalent $Ni^{2+}/Cu^{2+}/Fe^{2+}$ ions, resulting in a series of novel TM-cluster-substituted POTs.[4] The introduction of tri/tetravalence TM ions, like Cr^{3+}, Ti^{4+}, and Zr^{4+} ions, into the above reaction systems has also greatly attracted our interest. On the other hand, the P-/Si-centered fragments are usually used as the precursors in the most of the known Zr-substituted POTs, but only few Ge-centered fragments are used as the precursors. If Ge-centered precursor reacts with Zr-salt, can the high-nuclear Zr-cluster substituted POTs be made? Considering the above-mentioned reasons and inspirations from our previous work, the trilacunary $[A\text{-}\alpha\text{-}GeW_9O_{34}]^{10-}$ fragment was chosen as the precursor to make Zr-substituted POTs (Supporting Information, Scheme S1). Fortunately, a Zr24-cluster substituted

poly(POT), $Na_{10}K_{22}[Zr_{24}O_{22}(OH)_{10}(H_2O)_2(W_2O_{10}H)_2$-$(GeW_9O_{34})_4(GeW_8O_{31})_2]\cdot85H_2O$ $(Na_{10}K_{22}\cdot\mathbf{1}\cdot85H_2O)$, has been synthesized. **1** has the largest $[Zr_{24}O_{22}(OH)_{10}(H_2O)_2]$ (Zr_{24}) cluster in all the Zr-based POTs up to date, in which the Zr_{24} cluster was trapped by different fragments of B-α-GeW_9O_{34} (B-GeW_9), B-α-GeW_8O_{31} (B-GeW_8), and W_2O_{10} (W_2). Moreover, the oxygenation reaction of thioethers by H_2O_2 is chosen as an object due to the importance in organic chemistry. Results indicate that **1** is an effective catalyst during the course of oxygenation of thioethers. We believe that the unique redox property of oxygen-enriched POT fragments and the Lewis acidity of the Zr cluster imbedded in **1** provide a sufficient driving force for the catalytic conversion from thioethers to sulfoxides/sulfones, which can be consolidated by our experiments (vide infra) and the fact that neither thioethers nor sulfoxides are rapidly oxidized by the oxidants at room temperature in the absence of catalysts, although the oxidation of thioethers to the corresponding sulfoxides as well as oxidation of the sulfoxides to the corresponding sulfones by H_2O_2 is thermodynamically favorable.[5]

■ RESULTS AND DISCUSSION

Structural Description. Colorless crystals of $Na_{10}K_{22}\cdot\mathbf{1}\cdot85$ H_2O were made by the hydrothermal reaction of $[A$-α-$GeW_9O_{34}]^{10-}$ (A-GeW_9), $ZrOCl_2\cdot8H_2O$ and Na_2CO_3 (Their molar ratio is 0.32:0.62:0.40) in sodium acetate buffer at 200 °C for 3 days. Though the A-GeW_9 fragment was used as the starting material, **1** (Figure 1a) contains B-GeW_9 and B-GeW_8 units (Figure 1b), indicating that the isomerization of A-GeW_9 $\rightarrow$ B-GeW_9 and the degradation of B-GeW_9 $\rightarrow$ B-GeW_8 must have taken place during the course of the reaction; that is, the isomerization is prior, and the degradation is hind (Figure S1, Supporting Information). As shown in Figure 1a, **1** includes four B-GeW_9, two B-GeW_8, and two W_2O_{10} units, showing that

Figure 1. (a) Structures of the hexamer **1**.;(b) isomerization of the A-GeW_9 ion, and the degradation of the B-GeW_9 fragment, as well as the formation of the W_2O_{10} group. Color codes: O, red; Zr, green.

the isomerized B-GeW_9 frag-ments were partially degraded to the B-GeW_8 segments. As to A- and B-GeW_9, the latter is more stable than the former, which has been confirmed by the above isomerization of A-GeW_9 $\rightarrow$ B-GeW_9. The rational reason is that the A-GeW_9 has six exposed surface O atoms at its trivacant site, while the B-GeW_9 owns seven such O atoms, which results in that the B-GeW_9 as a heptadentate ligand can better enhance the stability of the products than the A-GeW_9 as a hexadentate ligand when they chelated to the in situ formed Zr cluster. The B-GeW_8 segment is a tetra-lacunary Keggin unit and derived from the degradation of B-GeW_9 by removing a WO_6 group. As to the W_2O_{10} dimer formed by two edge-sharing WO_6 octahedra, it can be understood as the congregation of two degradative WO_6 groups. In our previous study, the degradative WO_6 groups from the $[A$-α-$PW_9O_{34}]^{9-}$ precursor can reconstruct the tetratungstate W_4O_{16} core made up of four edge-sharing WO_6 octahedra.[4e] The W_4O_{16} core can be viewed as the fusion of two W_2O_{10} moieties by sharing two edges.

The experimental powder X-ray diffraction (PXRD) pattern of **1** is consistent with the simulated pattern derived from the single crystal X-ray diffraction data, indicating the good purity of the sample phase (Figure S2, Supporting Information). X-ray structure analysis reveals that **1** is a centrosymmetric Zr_{24}-cluster hexamer $[Zr_{24}O_{22}(OH)_{10}(H_2O)_2(W_2O_{10}H)_2$-$(GeW_9O_{34})_4(GeW_8O_{31})_2]^{32-}$ (Figures 1a and 2a), which consists of two symmetry-related **1a** trimers $[Zr_{12}O_{11}(OH)_5$-$(H_2O)(W_2O_{10}H)(GeW_9O_{34})_2(GeW_8O_{31})]^{16-}$ (Figure 2b) via six μ_3-oxo bridges. Twelve OH bridges and two coordination water molecules O(126,126A) in **1** are localized by bond valence sum (BVS) calculations (Table S1, Supporting Information).[6a,b] **1** displays two remarkable features: the coexistence of three POT fragments, namely, GeW_8, GeW_9, and W_2 and the occurrence of an unprecedented S-shaped giant Zr_{24} cluster (Figure 2c and Supporting Information Figure S3) that is incorporated to the skeleton of **1** and stabilized by six mixed lacunary fragments and two W_2O_{10} segments. In the Zr_{24} cluster, interestingly, $Zr(2,4-12)$ ions form an edge-sharing dioctahedral distribution fashion and $Zr(1,3)$ ions are situated on both sides of the edge-sharing dioctahedron (Figure 3). Notably, the $W(1,2)$ and $Zr(1,2)$ atoms illustrate the distribution motif of a truncated cubane with an appended Zr2 atom (Figure 2d), which is somewhat similar to the appended Mn_4O_4 core with an appended Mn ion in $[Mn^{III}_2Mn^{II}_4(\mu_3$-$O)_2(H_2O)_4(B$-$\beta$-$SiW_8O_{31})(B$-$\beta$-$SiW_9O_{34})(\gamma$-$SiW_{10}O_{36})]^{18-}$ reported by Cronin et al.[6c] **1a** is constructed from three Zr-substituted Keggin-type POT units **1aa**, **1ab**, and **1ac** via the bridging O/OH, $Zr(1,2)$, and $W(1,2)$ atoms. **1aa**, **1ac**, and **1ab** can be viewed as two tri-Zr substituted GeW_9 units and one penta-Zr substituted GeW_8 unit. **1aa** is a trilacunary GeW_9 unit capped by a Zr_3 core made of $Zr(7-9)$ atoms via a corner-sharing μ_4-O atom (Figure 2e). The Zr7 ion is eight-coordinated, while $Zr(8,9)$ ions are seven-coordinated (Figure S4a,b, Supporting Information). **1ac** is also a trilacunary GeW_9 unit capped by a Zr_3 core built by $Zr(10-12)$ ions (Figure 2g). But the obvious difference from **1aa** is that **1ac** contains a seven-coordinated Zr10 ion and two eight-coordinated $Zr(11, 12)$ ions (Figure S4e,f, Supporting Information). **1ab** is a tetralacunary GeW_8 unit capped by a Zr_5 cluster built by $Zr(3-7)$ ions (Figure 2f). The $Zr(5-7)$ ions are located at the trilacunary sites, the Zr3 ion is encapsulated to the fourth lacunary site of GeW_8 unit while the Zr4 ion caps on the window surrounded by $Zr(3,5,6)$ ions
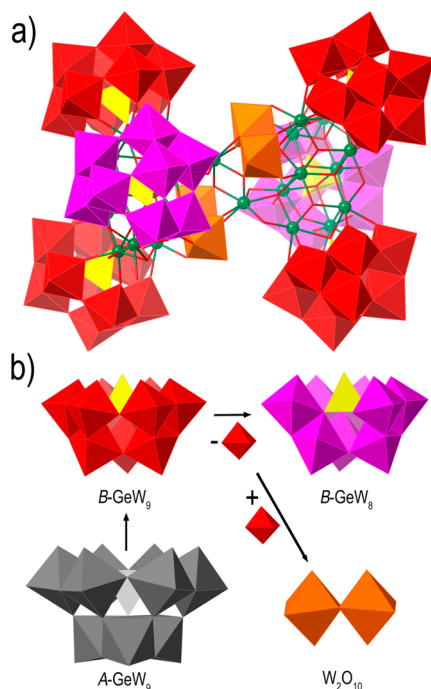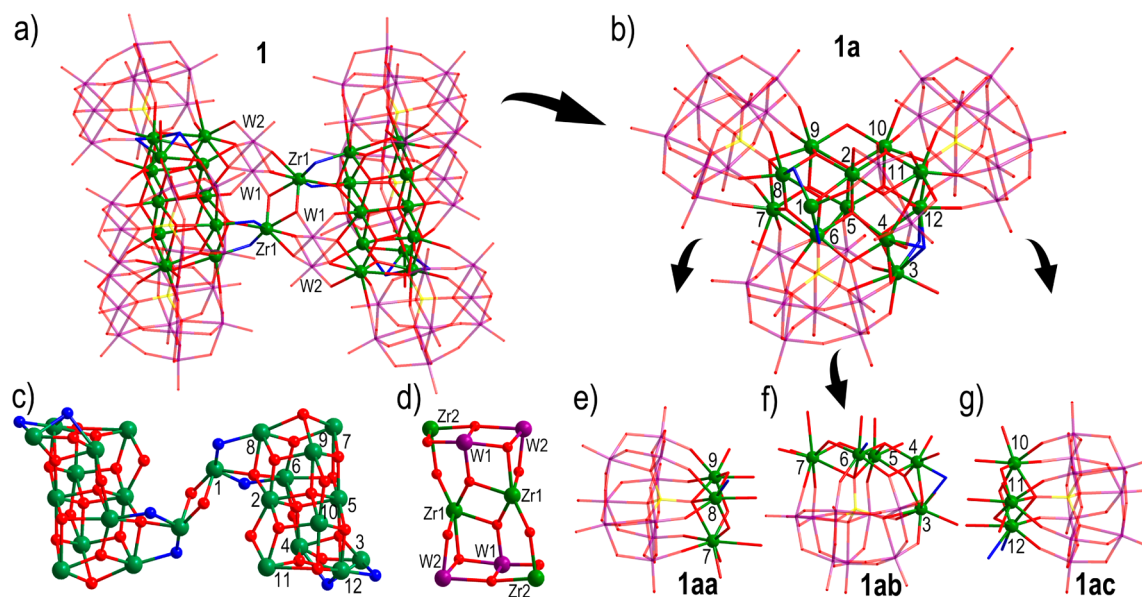
Figure 2. Ball-and-stick representations of the (a) polyanion **1**, (b) trimer **1a**, (c) the Zr_{24} cluster in **1**, (d) the distribution motif of W1, W2, Zr1, and Zr2 atoms, (e, f, and g) three Zr-substituted Keggin-type POT units in **1a**. Color codes: O, red; OH, blue; W, purple; Ge, yellow, Zr, green.
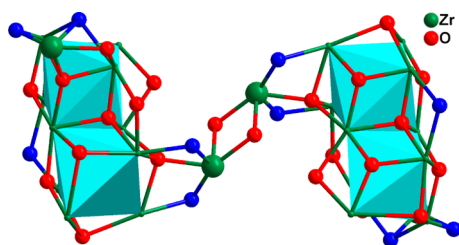
Figure 3. Alignment of 24 the Zr ions of the Zr_{24}-cluster in **1**. Color code: blue, hydroxyl atoms.

through two μ_3-O and two μ_4-O atoms. The Zr3 ion is eight-coordinated and the remaining Zr(4−6) ions are seven-coordinated (Figure S4c,d, Supporting Information). It should be pointed out that the Zr7 ion simultaneously occupies the defect sites of **1aa** and **1ab**. Notably, 12 crystallographically independent Zr ions show three different coordination geometries: Zr(1,2,4,5,9,10) ions display the distorted monocapped octahedra, Zr(3,7,11,12) ions adopt the distorted bicapped trigonal prisms, and Zr(6,8) ions reside in the distorted monocapped trigonal prisms (Figure S5, Supporting Information).

Another interesting feature of **1** is that there are two pairs of intriguing triangular atom alignments (Figure 4): one is composed of the Zr(2,4,6,8,11) and W21 atoms, and this linking mode resembles the Ni_6 clusters observed in $[Ni(enMe)_2]_3[H_6Ni_{20}P_4W_{34}(OH)_4O_{136}(enMe)_8(H_2O)_6]\cdot12H_2O^{4e}$ and $[Ni(en)_2(H_2O)_2]_6\{Ni_6(Tris)(en)_3(BTC)_{1.5}(B\text{-}\alpha\text{-}PW_9O_{34})\}_8\cdot12en\cdot54\ H_2O;^{4f}$ the other contains the Ge(1−3), Zr(3,5,7,9,10,12), and W26 atoms, and the Zr5 atom is inside the triangle, so that the linking mode is unobserved. Two triangles are connected each other via a μ-O, six μ_3-O, and seven μ_4-O atoms. It is notable that the Zr1 ion cannot be located in the POM skeleton pocket, and it plays a crucial role in linking two symmetry-related Zr_{12} cores to form the unprecedented S-shaped Zr_{24} cluster. In the solid state, **1** is stabilized by Na^+ and K^+ countercations, which are closely associated with the cluster polyanions. In the packing
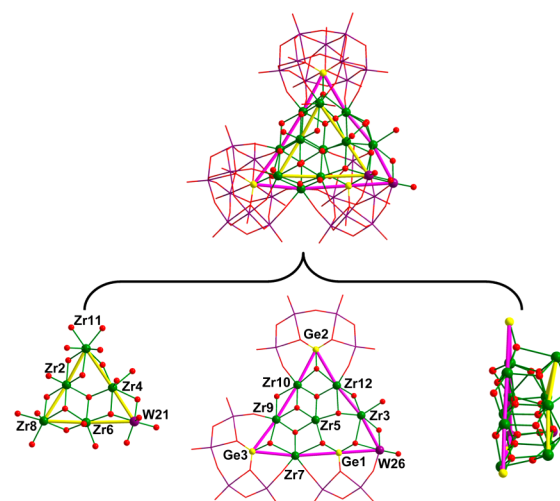
Figure 4. Two pairs of triangular alignments.

arrangement in the *bc* plane, cluster polyanions are arranged in the −AAA− fashion (Figure S6, Supporting Information).

In addition, similar to **1**, other TM-substituted germanotungstates containing GeW_9 and GeW_8 fragments have been observed in $[Cu_3(H_2O)(B\text{-}\beta\text{-}GeW_9O_{33}(OH))(B\text{-}\beta\text{-}GeW_8O_{30}(OH))]^{12-}$ (**2a**), $[Co(H_2O)_2\{Co_3(B\text{-}\beta\text{-}GeW_9O_{33}(OH))(B\text{-}\beta\text{-}GeW_8O_{30}(OH))\}_2]^{22-}$ (**2b**), $[Mn(H_2O)_2\{Mn_3(H_2O)(B\text{-}\beta\text{-}GeW_9O_{33}(OH))(B\text{-}\beta\text{-}GeW_8O_{30}\ (OH))\}_2]^{22-}$ (**2c**) (Figure S7a, Supporting Information)[7] and $[Cu_{10}(H_2O)_2(N_3)_4(GeW_9O_{34})_2(GeW_8O_{31})_2]^{24-}$ (**3**) (Figure S7b, Supporting Information).[8] However, the most remarkable differences between **1**, **2**, and **3** lie in three aspects: (a) GeW_9 and GeW_8 fragments in **1** are $B\text{-}\alpha$-configuration while those in **2** and **3** are $B\text{-}\beta$-configuration; (b) **1** was made under hydrothermal conditions by means of the $A\text{-}\alpha\text{-}GeW_9$ precursor and the transformation pathway from $A\text{-}\alpha\text{-}GeW_9$ to $B\text{-}\alpha\text{-}GeW_9$ and $B\text{-}\alpha\text{-}GeW_8$ occurred, whereas **2** and **3** were made by the $[\gamma\text{-}GeW_{10}O_{36}]^{8-}$ precursor and the evolution of $[\gamma\text{-}GeW_{10}O_{36}]^{8-}$ to $B\text{-}\beta\text{-}GeW_9$ and $B\text{-}\beta\text{-}GeW_8$ happened; (c) the number of TM centers in **1** is much larger than those in **2** and **3**. A comparison

of **1** with **2** and **3** shows that the number of the TM cations incorporated by POM skeletons increases when the number of the lacunary POM units increases. For example, three Cu/Co/Mn ions are contained in **2** when the number of lacunary POM units is two and 10 Cu ions in **3** when the number of lacunary POM units is four. With regard to **1**, the number of lacunary POM units is elevated to six, and 24 Zr cations are trapped. Additionally, in comparison with previously reported POT aggregates with over 24 TM ions such as $[H_{56}Fe_{28}P_8W_{48}O_{248}]^{28-}$ (**Fe₂₈**),[2b] $[(P_8W_{48}O_{184})\{(P_2W_{14}Mn^{III}_4O_{60})(P_2W_{15}Mn^{III}_3O_{58})_2\}_4]^{152-}$ (**Mn₄₀**),[2g] $[(NH_4)_{20}\{(W)W_5O_{21}(SO_4)\}_{12}\{(Fe^{III}(H_2O))_{30}\}(SO_4)_{13}(H_2O)_{34}]]^{12-}$ (**Fe₃₀**),[2h] and $[\{Ni^{II}_6(Tris)(en)_3(BTC)_{1.5}(B-\alpha-PW_9O_{34})\}_8]^{36-}$ (**Ni₄₈**),[2i] several obvious discrepancies can be found: (i) the tetravalence Zr^{4+} ions are introduced to **1** while the chemical valences of TM ions in **Fe₂₈**, **Mn₄₀**, **Fe₃₀**, and **Ni₄₈** are lower than 4; (b) **1**, **Fe₂₈**, **Mn₄₀**, **Fe₃₀**, and **Ni₄₈** consist of three (trivacant B-GeW₉, tetravacant B-GeW₈, W₂), one (hexavacant P_2W_{12}), three (trivacant P_2W_{15}, tetravacant P_2W_{14}, multivacant P_8W_{48}), one ($\{(W)W_5\}$), and one (trivacant B-PW₉) POT units, respectively; (c) to reduce the steric hindrance, the POT units in them are not coplanar and exhibit different spatial alignments; (d) **1** and **Ni₄₈** are hydro-thermally made, whereas the remaining are synthesized in conventional aqueous conditions. From the above we can see that the introduction of multivacant POT fragments (i.e., P_2W_{12}, P_8W_{48}) and anionic components (i.e., SO_4^{2-}, Tris, BTC) can effectively increase the number of TM ions in the products, which offer us great enlightenment in the preparations of much higher TM-substituted POMs.

Catalytic Oxidation. The catalytic oxidations of organic compounds under mild conditions are of both considerable intellectual interest and potential utility.[9] Catalytic oxidation of organic sulfide remains a topical interest owing to the versatile utility of both sulfoxide and sulfone in organic synthesis.[10] While a plethora of oxygen donors are available, utilization of "green" oxygen donors such as H_2O_2 has become increasingly prominent.[11] According to the previous reports,[12] thioethers can be efficiently oxidized by H_2O_2 in the presence of titanopolytungstates to produce the corresponding oxygenated products (sulfoxides, RR′SO and sulfones, RR′SO₂) in practically quantitative yield based on both H_2O_2 and substrate consumed (Scheme 1). Because Zr and Ti belong to the same

Scheme 1. Catalytic Oxidation of Thioethers

$$R-S-R' + H_2O_2 \xrightarrow[CH_3CN]{Na_{10}K_{22}\cdot\mathbf{1}\cdot85H_2O} \underset{(RR'SO)}{R-\overset{O}{\underset{}{S}}-R'} + \underset{(RR'SO_2)}{R-\overset{O}{\underset{O}{S}}-R'} + H_2O$$

(RR′S)

group in the periodic table of elements, using $Na_{10}K_{22}\cdot\mathbf{1}\cdot85H_2O$ as a catalyst, catalytic oxidations of various thioethers with H_2O_2 have been successfully achieved and give rise to the corresponding oxygenated products. Products were identified by GC–MS spectra. The selectivity of sulfoxide and sulfone products and the conversion of initial sulfides were quantified by GC spectra. Table 1 and Table S2 (Supporting Information) summarize the reactivity data for oxidation of 11 representative thioethers in MeCN at room temperature/60 °C in the presence of $Na_{10}K_{22}\cdot\mathbf{1}\cdot85H_2O$ and in the absence of $Na_{10}K_{22}\cdot\mathbf{1}\cdot85H_2O$, respectively.

As we can see in Table S2, most of the oxidation reaction can happen in the absence of $Na_{10}K_{22}\cdot\mathbf{1}\cdot85H_2O$, but the conversion and selectivity of the majority of catalytic oxidation reactions

Table 1. Results for Oxygenation of Various Thioethers with 30% H_2O_2 Catalyzed by $Na_{10}K_{22}\cdot\mathbf{1}\cdot85H_2O$ in MeCN

Entry	Substrate	Time (h)	Temp. (°C)	Conv. (%)[a]	Selectivity (%) RR′SO	RR′SO₂
1[b]	(dipropyl sulfide)	1	25	91	0	100
2	(dibenzyl sulfide)	1	25	89	0	100
3[c]	(Ph–SCH₃)	1	60	99	16	84
4	(Ph–S–CH₂CH₂OH)	1	60	100	0	100
5	(H₃CO–C₆H₄–SCH₃)	1	60	100	0	100
6	(SCH₃, OCH₃)	1	60	100	8	92
7	(OCH₃, SCH₃)	1	60	98	64	36
8	(CH₃–C₆H₄–SCH₃)	1	60	100	8	92
9	(Br–C₆H₄–SCH₃)	1	60	100	3	97
10	(Br, SCH₃)	1	60	100	13	87
11	(SCH₃, Br)	1	60	69	90	10
12	(NO₂–C₆H₄–SCH₃)	1	60	100	10	90
13	(SCH₃, NO₂)	1	60	77	50	50
14	(diphenyl sulfide)	2	60	45	73	27
15	(dibenzothiophene)	2	60	trace	—	—

[a]The conversion based on substrate consumed. [b]Reaction conditions for the entries 1 and 2: substrate, 0.5 mmol; H_2O_2, 1 mmol; $Na_{10}K_{22}\cdot\mathbf{1}\cdot85H_2O$, 0.5 × 10⁻² mmol; MeCN10, mL. [c]Reaction conditions for entries 3 to 16: substrate, 0.5 mmol; H_2O_2, 1.5 mmol; $Na_{10}K_{22}\cdot\mathbf{1}\cdot85H_2O$, 0.5 × 10⁻² mmol; MeCN, 10 mL.

are very low. Among all the reactions, entry 6 has the highest conversion, which is just about 23%. However, in the presence of $Na_{10}K_{22}\cdot\mathbf{1}\cdot85$ H_2O as a catalyst to activate H_2O_2, the conversion and selectivity are greatly improved, indicating that $Na_{10}K_{22}\cdot\mathbf{1}\cdot85$ H_2O is an effective catalyst for oxygenation of thioethers by H_2O_2 (Table 1). Particularly, entries 4 and 5 manifest the formation of 100% sulfone. The introduction of electron-donating groups on the aromatic ring of aryl–alkyl thioethers (entries 5–8) gave a higher ratio of sulfone than the introduction of electron-withdrawing groups (entries 9–13). It was also found that the position property of the substituents of aryl–alkyl thioethers (entries 3–13) should affect the ratio of sulfone and sulfoxide and the ortho-substituent groups increased the conversion of sulfoxide. Additionally, the steric hindrance effect of aryl–aryl thioethers has an obvious influence on the conversion of oxygenated products (entries 14–15) and the large steric hindrance produces a lower-conversion.

To check the recyclability of the heterogeneous catalyst $Na_{10}K_{22}\cdot\mathbf{1}\cdot85H_2O$, entry 5 worked as an example for investigation. Additional substrate and H_2O_2 were added into the reaction mixture when the previous run was completed. The results exhibit that the catalytic activity was not obviously changed after six-run duplicate operations (Table S3,

Supporting Information). The catalyst can be easily recovered from the solvent/oxidant/substrate system by filtration upon completion of the sixth run. The recovery percent reached up to 98%, and the filtrate showed negligible reactivity when extra substrate and H_2O_2 were added into it. According to the comparisons of IR spectra (Figure S8, Supporting Information) and PXRD patterns (Figure S10, Supporting Information) of the fresh catalyst and the recovered catalyst after the sixth-run reaction, the structural integrity of the recovered catalyst was still retained. The reason for some trivial differences in IR and PXRD spectra may be that the recovered catalyst has been partly peroxidated by H_2O_2. The comparisons of IR spectra of the fresh catalyst and that of the catalysts after first-run reaction for entries 3, 8, 11, and 14 are shown in Figure S9 (Supporting Information). In comparison with previous reported results,[10c,13] $Na_{10}K_{22} \cdot \mathbf{1} \cdot 85H_2O$ displays comparatively better catalytic activities toward oxidations of thioethers under similar conditions. For example, for the oxidation of thioanisole (entry 3) with $Na_{10}K_{22} \cdot \mathbf{1} \cdot 85H_2O$ as a catalyst, the conversion was 99% and the turnover frequency (TOF) was 99 h^{-1} at 60 °C, which are slightly higher than those (conversion: 92%, TOF: 38 h^{-1}) using $[\gamma\text{-}1,2\text{-}H_2SiV_2W_{10}O_{40}]/SiO_2$ as a catalyst at 20 °C.[13a] As to entry 3, when $MnSO_4 \cdot H_2O$ catalyst and 3 equiv H_2O_2 were utilized and the reaction time was prolonged to 24 h, although the conversion was up to 100%, the selectivities to sulfone and sulfoxide were 57% and 43%, respectively.[13b] Similarly, with regard to entry 3, employing 2,6-bis(acetylamino)pyridine and 2,6-bis(3-{4-[3,5-bis(phenylmethoxy)phenylmethoxy]phenyl}-propanoylamino)pyridine as catalysts with 2.5 equiv H_2O_2 at 30 °C gave a time of flight (TOF) of 6.8 h^{-1} and 16 h^{-1}, respectively.[13c] In the case of entry 14, when $(Bu_4N)_4[\gamma\text{-}SiW_{10}O_{34}(H_2O)_2]$ worked as a catalyst with 1 equiv of H_2O_2 without an additional additive, the conversion of phenyl sulfide to the sulfoxide is tardy at 23 °C, generating only 38% after 3 h.[10c] Overall, the catalytic oxidation of thioethers in this work may be potentially useful for the removal of organic sulfur content.

CONCLUSIONS

An unprecedented Zr_{24}-cluster substituted poly(POT) $Na_{10}K_{22} \cdot \mathbf{1} \cdot 85H_2O$ has been successfully made under hydrothermal conditions and contains the largest $[Zr_{24}O_{22}\text{-}(OH)_{10}(H_2O)_2]$ cluster in POM chemistry. More interestingly, the Zr_{24} cluster was simultaneously trapped by inequivalent fragments of $B\text{-}GeW_9$, $B\text{-}GeW_8$, and W_2. The formation of an $Na_{10}K_{22} \cdot \mathbf{1} \cdot 85H_2O$ not only exemplifies the possibility that more giant Zr-clusters can be incorporated to lacunary POT skeletons, but also suggests the potential of combination of Zr^{4+} cations with other vacant POT fragments to create novel Zr-cluster-based POM materials in the rapid expansion and development era of POM chemistry. Moreover, catalytic oxidations of various thioethers by H_2O_2 using $Na_{10}K_{22} \cdot \mathbf{1} \cdot 85H_2O$ as a catalyst have been evaluated. In comparison with previous reported results,[10c,13] $Na_{10}K_{22} \cdot \mathbf{1} \cdot 85H_2O$ can be viewed as an effective catalyst for oxygenation of thioethers by H_2O_2 and may have the potential for the removal of organic sulfur content. In the following work, more catalytic reactions and relevant catalytic mechanism will be explored and developed. The isolation of this large-Zr-cluster substituted poly(POT) confirms that the combination of the hydrothermal technique, lacunary POTs, and TM cations with larger ionic radius, high positive charges, and high-coordination number can provide an effective strategy for making large or supralarge TM-cluster substituted poly-(POT)s. Cooperative actions between Zr^{4+} ions and POT components might potentially improve catalytic activities exemplified by oxygenation of thioethers by H_2O_2. The key points of the synthetic procedures have been well established. Further work with the aim of making novel poly(POT)s with special functionalities is in progress by making use of the reactions of those TM/lanthanide cations with the larger ionic radii and high-coordination numbers with multilacunary POTs or mixed multivacant POTs under hydrothermal conditions. Furthermore, some functional organic ligands will be introduced to this system to prepare novel organic−inorganic hybrid high-nuclear Zr/lanthanide substituted POT aggregates. It can be believed that this finding is very important in exploring the syntheses of large or supralarge TM-cluster substituted poly(POT)s.

■ EXPERIMENTAL SECTION

Physical Measurements. $K_8Na_2[A\text{-}\alpha\text{-}GeW_9O_{34}] \cdot 25H_2O$ was prepared by a literature method.[14] All other chemicals employed in this study were analytical reagent. H elemental analysis was carried out with a Vario EL III elemental analyzer. IR spectra (KBr pellets) were recorded on an ABB Bomen MB 102 spec-trometer. PXRD patterns were collected on a Bruker D8 Advance XRD diffractometer using Cu $K\alpha$ radiation. Thermogravimetric analysis was performed in a dynamic air atmosphere with a heating rate of 10 °C/min using a Mettler TGA/SDTA 851^e thermal analyzer. GC spectra were carried out with a Varian 430-GC gas chromatograph. GC−MS spectra were obtained from a Varian 450-GC/240-MS gas chromatograph−mass spectrometer.

X-ray Crystallography. A suitable single crystal was selected under an optical microscope and mounted onto the end of a thin glass fiber using cyanoacrylate adhesive. The intensity data were collected on a Mercury CCD diffractometer with graphite-monochromated Mo $K\alpha$ radiation ($\lambda = 0.71073$ Å) at room temperature. All absorption corrections were performed by using the SADABS program. The structure was solved by direct methods and refined by full-matrix least-squares on F^2 using the SHELXTL-97 program package.[15] ICSD-425690 contains the supplementary crystallographic data for this paper. These data can be obtained free of charge from the ICSD database via http://www.fiz-karlsruhe.de/request. Crystal data: $H_{186}Ge_6K_{22}Na_{10}O_{337}W_{56}Zr_{24}$, $M_r = 19590.01$, triclinic, $P\bar{1}$, $a = 17.1764(4)$, $b = 20.7259(6)$, $c = 23.1192(5)$ Å, $\alpha = 67.465(2)°$, $\beta = 76.759(2)°$, $\gamma = 73.217(2)°$, $V = 7212.6(3)$ Å^3, $Z = 1$, $\rho_{calcd} = 4.510$ g cm^{-3}, $\mu = 24.131$ mm^{-1}, $F(000) = 8706$, GOF = 1.059. A total of 70793 reflections were collected, 25299 of which were unique ($R_{int} = 0.0634$). $R_1/wR_2 = 0.0498/0.1222$ for 1849 parameters and 20748 reflections ($I > 2\sigma(I)$).

Synthesis for $Na_{10}K_{22} \cdot \mathbf{1} \cdot 85H_2O$. $K_8Na_2[A\text{-}\alpha\text{-}GeW_9O_{34}] \cdot 25H_2O$ (1.0 g, 0.32 mmol) and $ZrOCl_2 \cdot 8H_2O$ (0.2 g, 0.62 mmol) were stirred in 8 mL of 0.5 mol·L^{-1} sodium acetate buffer (pH = 4.8), and then Na_2CO_3 (1 mol·L^{-1}, 0.4 mL) was dropwise added under continuous stirring for 20 min. The resulting solution was sealed in a 35 mL stainless steel reactor with a Teflon liner and heated at 200 °C for 3 days and then cooled to room temperature. Colorless prismatic crystals of **1** were obtained. Yield: 0.23 g (45%) for **1** based on $ZrOCl_2 \cdot 8H_2O$. Elemental analysis (%) calcd for **1**: H, 0.96; Na, 1.17; K, 4.39; Ge, 2.22; Zr, 11.18; W, 52.55. Found: H, 0.88; Na, 1.00; K, 4.59; Ge, 2.56; Zr, 10.97; W, 52.24. IR (KBr, cm^{-1}): 3406 m, 1621 s, 965 s, 903 m, 766 w, 713 w, 459 m.

Experimental Procedure of Catalytic Oxidation of Various Thioethers with H_2O_2 Catalyzed by $Na_{10}K_{22} \cdot \mathbf{1} \cdot 85H_2O$. The catalytic oxidation of various thioethers was carried out in 25 mL glass vessel under vigorous agitation with a magnetic stirring bar at ambient temperature (25 °C) or heated (60 °C) at reflux. A desired amount of solid catalyst was placed into the glass vessel, then a solution containing thioether, acetonitrile, and dodecane (an internal standard for GC-analysis) was added. The reaction vessel was sealed and stirred at 25 °C or placed into a thermostated oil-bath (60 °C).

7641

dx.doi.org/10.1021/ja413134w | J. Am. Chem. Soc. 2014, 136, 7637−7642

After the reaction, the vessel was cooled to room temperature and diluted with ether for GC analysis. The thioether oxidation products (sulfoxide and sulfone) were identified with GC−MS and quantified using gas chromatography with internal standard techniques.

Recyclability of the catalyst: the oxidation of methyl 4-methoxyphenyl sulfide (entry 5 in Table 1) was selected as a probe reaction. At first, 0.5 mmol of methyl 4-methoxyphenyl sulfide, 1.5 mmol of H_2O_2, and 0.5×10^{-2} mmol of $Na_{10}K_{22} \cdot \mathbf{1} \cdot 85H_2O$ were added into 10 mL of MeCN. The mixture was stirred 1 h at 60 °C. Upon the completion of the reaction, another 0.5 mmol of methyl 4-methoxyphenyl sulfide and 1.5 mmol of H_2O_2 were added. After that, the mixture was stirred 1 h at 60 °C again. The process was repeatedly carried out.

Determination of Lattice Water Molecules. Lattice water molecules are located in the interspaces of cluster polyanions. $Na_{10}K_{22} \cdot \mathbf{1} \cdot 85H_2O$ is highly hydrated, and when it is exposed to the X-ray beam for the collection of intensity data, the water molecules of crystallization are easily lost from the structure. Therefore, some water molecules of crystallization cannot be directly determined by X-ray diffraction. A combination of elemental analysis and thermogravimetric analysis (Figure S11, Supporting Information) confirms the number of water molecules of crystallization in $Na_{10}K_{22} \cdot \mathbf{1} \cdot 85H_2O$, which is not uncommon in giant poly(POM) species.[16]

■ ASSOCIATED CONTENT

Ⓢ Supporting Information

Synthesis, BVS, catalysis, detailed structure description, TG, and IR. This material is available free of charge via the Internet at http://pubs.acs.org.

■ AUTHOR INFORMATION

Corresponding Author

ygy@fjirsm.ac.cn; zhaojunwei@henu.edu.cn

Notes

The authors declare no competing financial interest.

■ ACKNOWLEDGMENTS

■ REFERENCES

(1) (a) Kozhevnikov, V. *Catalysts for Fine Chemical Synthesis—Catalysis by Polyoxometalates*; John Wiley and Sons: Chichester, UK, 2002; p 117. (b) Topical issue on polyoxometalates, (Guest Ed.: Hill, C. L.), *Chem. Rev.* **1998**, *98*, 1. (c) *Polyoxometalate Chemistry: From Topology via Self-Assembly to Applications*; Pope, M. T., Müller, A., Eds.: Kluwer: Dordrecht, The Netherlands, 2001. (d) Rosnes, M. H.; Musumeci, C.; Pradeep, C. P.; Mathie-son, J. S.; Long, D.-L.; Song, Y.-F.; Pignataro, B.; Cogdell, R.; Cronin, L. *J. Am. Chem. Soc.* **2010**, *132*, 15490. (e) Zheng, S.-T.; Yang, G.-Y. *Chem. Soc. Rev.* **2012**, *41*, 7623. (f) Oms, O.; Dolbecq, A.; Mialane, P. *Chem. Soc. Rev.* **2012**, *41*, 7497.

(2) (a) Bassil, B. S.; Ibrahim, M.; Al-Oweini, R.; Asano, M.; Wang, Z. X.; Tol, J. V.; Dalal, N. S.; Choi, K. Y.; Biboum, R. N.; Keita, B.; Nadjo, L.; Kortz, U. *Angew. Chem., Int. Ed.* **2011**, *50*, 5961. (b) Godin, B.; Chen, Y.; Vaissermann, J.; Ruhlmann, L.; Verdaguer, M.; Gouzerh, P. *Angew. Chem., Int. Ed.* **2005**, *44*, 3072. (c) Lan, Y.; Bassil, B. S.; Xiang, Y.; Suchopar, A.; Powell, A. K.; Kortz, U. *Angew. Chem., Int. Ed.* **2011**, *50*, 4708. (d) Mal, S. S.; Kortz, U. *Angew. Chem., Int. Ed.* **2005**, *44*, 3777. (e) Kim, G. S.; Zeng, H. D.; VanDerveer, D.; Hill, C. L. *Angew. Chem., Int. Ed.* **1999**, *38*, 3205. (f) Sakai, Y.; Yoza, K.; Kato, C. N.; Nomiya, K. *Chem.—Eur. J.* **2003**, *9*, 4077. (g) Fang, X.; Kögerler, P.; Furukawa, Y.; Speldrich, M.; Luban, M. *Angew. Chem., Int. Ed.* **2011**, *50*, 5212. (h) Müller, A.; Diemann, E.; Kuhlmann, C.; Eimer, W.; Serain, C.; Tak, T.; Knöchel, A.; Pranzas, P. K. *Chem. Commun.* **2001**,

1928. (i) Zheng, S.-T.; Zhang, J.; Li, X.-X.; Fang, W.-H.; Yang, G.-Y. *J. Am. Chem. Soc.* **2010**, *132*, 15102.

(3) (a) Kikukawa, Y.; Yamaguchi, S.; Tsuchida, K.; Nakagawa, Y.; Uehara, K.; Yamaguchi, K.; Mizuno, N. *J. Am. Chem. Soc.* **2008**, *130*, 5472. (b) Fang, X.-K.; Anderson, T. M.; Hill, C. L. *Angew. Chem., Int. Ed.* **2005**, *44*, 3540. (c) Errington, R. J.; Petkar, S. S.; Middleton, P. S.; McFarlane, W. *J. Am. Chem. Soc.* **2007**, *129*, 12181. (d) Finke, R. G.; Rapko, B.; Weakley, T. J. R. *Inorg. Chem.* **1989**, *28*, 1573. (e) Bassil, B. S.; Dickman, M. H.; Kortz, U. *Inorg. Chem.* **2006**, *45*, 2394. (f) Bassil, B. S.; Mal, S. S.; Dickman, M. H.; Kortz, U.; Oelrich, H.; Walder, L. *J. Am. Chem. Soc.* **2008**, *130*, 6696. (g) Al-Kadamany, G.; Mal, S. S.; Milev, B.; Donoeva, B. G.; Maksimovs-kaya, R. I.; Kholdeeva, O. A.; Kortz, U. *Chem.—Eur. J.* **2010**, *16*, 11797.

(4) (a) Zheng, S.-T.; Yuan, D.-Q.; Jia, H.-P.; Zhang, J.; Yang, G.-Y. *Chem. Commun.* **2007**, 1858. (b) Zhao, J.-W.; Jia, H.-P.; Zhang, J.; Zheng, S.-T.; Yang, G.-Y. *Chem.—Eur. J.* **2007**, *13*, 10030. (c) Zhao, J.-W.; Wang, C.-M.; Zhang, J.; Zheng, S.-T.; Yang, G.-Y. *Chem.—Eur. J.* **2008**, *14*, 9223. (d) Zheng, S.-T.; Zhang, J.; Yang, G.-Y. *Angew. Chem., Int. Ed.* **2008**, *47*, 3909. (e) Zheng, S.-T.; Clemente-Juan, J. M.; Yuan, D.-Q.; Yang, G.-Y. *Angew. Chem., Int. Ed.* **2009**, *48*, 7176. (f) Li, B.; Zhao, J.-W.; Zheng, S.-T.; Yang, G.-Y. *Inorg. Chem.* **2009**, *48*, 8294.

(5) Gall, R. D.; Faraj, M.; Hill, C. L. *Inorg. Chem.* **1994**, *33*, 5015.

(6) (a) Brown, I. D.; Altermatt, D. *Acta Crystallogr.* **1985**, *B41*, 244. (b) Brese, N. E.; O'Keeffe, M. *Acta Crystallogr.* **1991**, *B47*, 192. (c) Mitchell, S. G.; Molina, P. I.; Khanra, S.; Miras, H. N.; Prescimone, A.; Cooper, G. J. T.; Winter, R. S.; Brechin, E. K.; Long, D.-L.; Cogdell, R. J.; Cronin, L. *Angew. Chem., Int. Ed.* **2011**, *50*, 9154.

(7) Nsouli, N. H.; Iamail, A. H.; Helgadottir, I. S.; Dickman, M. H.; Clemente-Juan, J. M.; Kortz, U. *Inorg. Chem.* **2009**, *48*, 5884.

(8) Zhang, Z.-M.; Qi, Y.-F.; Qin, C.; Li, Y.-G.; Wang, E.-B.; Wang, X.-L.; Su, Z.-M.; Xu, L. *Inorg. Chem.* **2007**, *46*, 8162.

(9) (a) Jørgensen, K. A. *Chem. Rev.* **1989**, *89*, 431. (b) Meunier, B. *Chem. Rev.* **1992**, *92*, 1411.

(10) (a) Fernandez, I.; Khair, N. *Chem. Rev.* **2003**, *103*, 3651. (b) Mikola-jaczyk, M.; Drabowicz, J.; Kielbasinski, P. *Chiral Sulfur Reagents: Applications in Symmetric and Stereoselective Synthesis*; CRC: Boca Raton, 1997. (c) Phan, T. D.; Kinch, M. A.; Barker, J. E.; Ren, T. *Tetrahedron Lett.* **2005**, *46*, 397.

(11) (a) Gresley, N. M.; Griffith, W. P.; Laemmel, A. C.; Nogueira, H. I. S.; Parkin, B. C. *J. Mol. Catal. A Chem.* **1997**, *117*, 185. (b) Carraro, M.; Nsouli, N.; Oelrich, H.; Sartorel, A.; Sorarù, A.; Mal, S. S.; Scorrano, G.; Walder, L.; Kortz, U.; Bonchio, M. *Chem.—Eur. J.* **2011**, *17*, 8371. (c) Kamata, K.; Hirano, T.; Kuzuya, S.; Mizuno, N. *J. Am. Chem. Soc.* **2009**, *131*, 6997. (d) Brégeault, J.-M.; Vennat, M.; Salles, L.; Piquemal, J.-Y.; Mahha, Y.; Briot, E.; Bakala, P. C.; Atlamsani, A.; Thouvenot, R. *J. Mol. Catal. A* **2006**, *250*, 177.

(12) (a) Kholdeeva, O. A.; Maksimov, G. M.; Maksimovskaya, R. I.; Kovaleva, L. A.; Fedotov, M. A.; Grigoriev, V. A.; Hill, C. L. *Inorg. Chem.* **2000**, *39*, 3828. (b) Gall, R. D.; Hill, C. L.; Walker, J. E. *Chem. Mater.* **1996**, *8*, 2523.

(13) (a) Kasai, J.; Nakagawa, Y.; Uchida, S.; Yamaguchi, K.; Mizuno, N. *Chem.—Eur. J.* **2006**, *12*, 4176. (b) Alonso, D. A.; Nájera, C.; Varea, M. *Tetrahedron Lett.* **2002**, *43*, 3459. (c) Imada, Y.; Kitagawa, T.; Iwata, S.; Komiya, N.; Naota, T. *Tetrahedron* **2014**, *70*, 495.

(14) (a) Bi, L.-H.; Kortz, U.; Nellutla, S.; Stowe, A. C.; van Tol, J.; Dalal, N. S.; Keita, B.; Nadjo, L. *Inorg.Chem.* **2005**, *44*, 896. (b) Haraguchi, N.; Okaue, Y.; Isobe, T.; Matsuda, Y. *Inorg. Chem.* **1994**, *33*, 1015.

(15) Sheldrick, G. M. *SHELXTL-97, Program for Crystal Structure Solution*; University of Göttingen: Germany, 1997.

(16) Mialane, P.; Dolbecq, A.; Marrot, J.; Rivière, E.; Sécheresse, F. *Angew. Chem., Int. Ed.* **2003**, *42*, 3523.

7642

dx.doi.org/10.1021/ja413134w | *J. Am. Chem. Soc.* 2014, 136, 7637−7642